

CHARACTERIZATION OF A NOVEL TOW-STEERED THIN PLY THERMOPLASTIC BOOM FOR SMALL SATELLITE MISSIONS

Christopher Schappi¹, Oleksandr Kravchenko

Mechanical and Aerospace Engineering, Old Dominion University, Norfolk, VA, 23529

Abstract

Deployable composite booms are important structural elements for enabling large-area subsystems in small satellite missions, including antennas, solar arrays, and sails. While many conventional designs use uniform fiber architectures, advances in automated fiber placement enable tow steering, allowing spatially varying stiffness distributions that improve structural performance. This study investigates the influence of fiber orientation on the dynamic, stability, and thermoelastic behavior of thin-ply thermoplastic lenticular booms using a finite element framework. Three representative geometries—(i) a flat laminate, (ii) a half-lenticular cross section, and (iii) a full lenticular cross section—are analyzed to examine the effects of curvature and cross-sectional closure.

Results show that axial fiber alignment produces the highest first-mode response in flat and open geometries, while the closed-section lenticular boom exhibits a shifted optimum, with peak response occurring at a small off-axis orientation. These configurations result in higher natural frequency and buckling load in the closed-section model, a trend consistent with increased coupling among axial, shear, and torsional stiffness contributions. Thermoelastic analysis shows that the closed cross section develops substantially lower thermally induced deformation than the open geometry. A tow-steered laminate architecture is then introduced and evaluated against uniform laminates, highlighting the importance of geometry–material coupling.

Introduction

The evolution of small satellite platforms has fundamentally transformed the landscape of space missions. Advances in the miniaturization of spaceflight hardware have enabled CubeSats and other small satellites to perform increasingly sophisticated tasks, ranging from Earth observation to deep-space technology demonstrations [1]. Despite these advancements, a critical limitation remains: many essential subsystems rely on physical size to achieve their intended function. Antennas require a large footprint as performance scales with aperture size, solar arrays depend on surface area for power generation, and solar sails rely on expansive geometries for propulsion

[2, 3]. As a result, deployable structures remain a key enabling technology for high-performance small satellite systems.

Deployable composite booms are widely used as structural elements to support these large-area systems as seen in Figure 1. Oxford Space System's wrapped-rib antenna utilizes carbon fiber lenticular ribs covered in a metal mesh reflector surface to provide a high-packing factor deployable antenna capable of being stowed about a center spool [4]. NASA's Advanced Composite Solar Sail System (ACS3) mission implemented four lenticular booms to support an 80 m² solar sail capable of being stowed within a 12U CubeSat bus [3]. CalTech's Space Solar Power Project (SSPP) leverages deployable longerons to support a large-area photovoltaic membrane that can store four 2 m long booms about a 200 mm diameter spool [5].

The ability of these booms to stow compactly and deploy reliably makes them attractive structures for modern spacecraft applications. However, many conventional boom designs rely on uniform fiber architectures, which can limit the extent to which the anisotropic behavior of composite materials is exploited. This restriction becomes increasingly significant in applications where stiffness, stability, and thermal behavior must be simultaneously optimized.

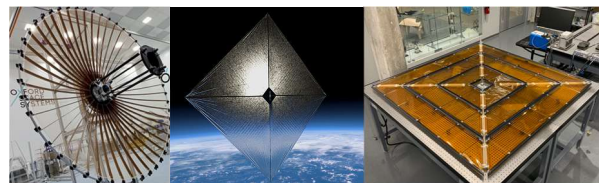


Figure 1. Oxford Space Systems wrapped-rib antenna (left), NASA's ACS3 solar sail (middle), and CalTech's SSPP deployable solar array (right) [1,2,3].

Automated Fiber Placement (AFP) techniques have introduced the capability to steer fiber tows along curvilinear paths, enabling spatially varying stiffness distributions within a structure [6]. When combined with thin-ply thermoplastic composites, which offer advantages such as improved damage tolerance, weldability, and reprocessability, tow steering presents a promising design paradigm for next-generation

deployable structures. However, the interaction between fiber orientation, structural geometry, and manufacturing-induced effects remains insufficiently understood – particularly for curved, thin-walled geometries such as lenticular booms.

This work seeks to address this gap by developing a multiphysics modeling framework to investigate how fiber orientation influences the structural and thermal behavior of deployable composite booms. Through systematic parametric studies, the relationship between fiber architecture and key performance metrics: (i) natural frequency, (ii) buckling resistance, and (iii) thermal deformation are examined. The results are then used to guide the design of tow-steered morphologies intended to be mechanically advantageous and compatible with manufacturable approaches.

Background

Deployable boom technologies have evolved significantly to meet the demands of modern space systems. Among the most widely used architectures are Triangular Rollable and Collapsible (TRAC) booms, Storable Extendible Tubular Members (STEM), and Collapsible Tubular Members (CTM) otherwise known as lenticular cross-section booms [7]. Each of these configurations offer distinct advantages and limitations in terms of stiffness, packaging efficiency, and deployment reliability. Figure 2 shows the geometry of TRAC, STEM, and CTM booms.



Figure 2. Deployable boom types: TRAC (left), STEM (middle), CTM/lenticular (right) [7].

Lenticular booms in particular have gained attention due to their ability to form a closed cross-section upon deployment. This closed geometry enhances bending and torsional stiffness while maintaining a low stowed volume [8]. Furthermore, the structural efficiency of lenticular configurations makes them well suited for applications requiring long-span deployable structures that must pack away into constrained launch volumes [7].

In parallel, thermoplastic composite materials have emerged as a promising alternative to traditional thermoset systems. Their ability to undergo melt processing enables faster manufacturing cycles and

supports advanced fabrication techniques such as AFP and thermostamping. Additionally, thermoplastics offer improved fracture toughness and potential for in-space manufacturing, making them highly attractive for future space systems [9].

Despite these advantages, current deployable boom designs largely rely on constant-stiffness laminates, where fiber orientations are uniform across the structure. This approach does not fully leverage the design freedom offered by AFP-based tow steering, where fiber orientations can be tailored to match local loading conditions. As a result, there exists an opportunity to significantly improve structural performance by integrating variable stiffness architectures into deployable boom design.

Modeling Approach

To investigate the influence of fiber orientation on structural performance of lenticular booms, a finite element model was developed in Abaqus CAE. Three geometries were considered: (i) a flat laminate representing a baseline case, (ii) a half-lenticular cross-section representing an open curved geometry, and (iii) a full lenticular cross-section representing a closed structural configuration.

The models were constructed using continuum shell elements to capture the thin-walled behavior of the composite structure while maintaining computational efficiency. Composite layups were defined with variable fiber orientations, which were systematically varied from $\pm 0^\circ$ to $\pm 90^\circ$ in increments of 10° with the inclusion of 45° . This parametric approach enabled the isolation of fiber orientation effects across the three geometries shown in Figure 3. Fiber orientations were defined with respect to the axial length of the geometry, with 0° and 90° defined as shown in Figure 4. Lastly, the models used the material properties in Table 1.

Table 1. Material properties

Property	Symbol	Value	Units
Longitudinal modulus	E_1	147000	MPa
Transverse modulus	E_2	8700	MPa
In-plane shear modulus	G_{12}	5200	MPa
Poisson's ratio	ν_{12}	0.32	
Density	ρ	1.55E-09	tonne/mm ³
Ply thickness	t	0.15	mm
Longitudinal coefficient of thermal expansion	α_1	9.00E-07	1/°C
Transverse coefficient of thermal expansion	α_2	2.2E-05	1/°C

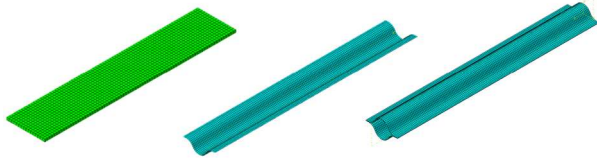


Figure 3. Laminate geometries: flat (left), half-lenticular (middle), full lenticular (right).

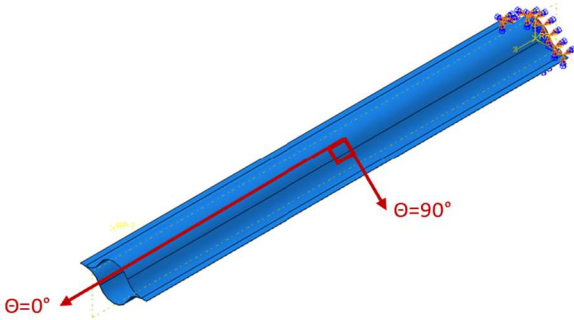


Figure 4. Fiber orientation definitions and fixed boundary condition.

The analysis framework incorporated three primary simulations: modal analysis to determine natural frequencies, linear buckling analysis to evaluate stability under compressive loading, and thermoelastic analysis to assess deformation resulting from thermal gradients associated with the fabrication process. The thermal analysis simulated the effects of the composites boom cooling down from processing temperature to ambient conditions, to estimate deformation associated with anisotropic thermal contraction.

To ensure the validity of the modeling approach, the baseline flat laminate model was compared to an analytical Timoshenko beam solution. The close agreement between analytical and numerical results provided evidence that the baseline model captured the dominant stiffness and mass characteristics of the flat laminate case.

Results and Discussion

Natural Frequency

The influence of fiber orientation on dynamic response was evaluated through eigenfrequency analysis for the three representative geometries seen in Figure 3. In all cases, a consistent cantilevered (fixed-free) boundary condition was applied to replicate the deployed configuration in which one end of the boom would be affixed to the satellite bus, with the other free in space. This fixed-free boundary condition can be seen in Figure

4, with the blue and orange arrows at one end of the boom denoting a fully constrained or fixed end.

Flat Laminate Beam

The flat laminate beam was used as a validation case to validate the mesh, composite layup, principal material direction definition, model parameters and establish baseline trends with respect to fiber orientation. The model consisted of a uniform rectangular cross section with a symmetric laminate layup. The results for this configuration, seen in Figure 5 below, are consistent with the expected trend for a beam whose bending response is dominated by longitudinal stiffness. The first natural frequency was maximized at $\pm 0^\circ$, where fibers aligned with the beam axis, resulting in the highest axial stiffness and bending rigidity. As the fiber orientation increased toward $\pm 90^\circ$, the first natural frequency experienced a nonlinear monotonic decrease consistent with a reduction in effective longitudinal stiffness. This behavior reflects the dominance of axial stiffness in governing bending response for flat laminates. It is important to note that the flat laminate beam is 200 mm in length, while both lenticular models are 330 mm in length. This means that while qualitative trends can be compared between the three geometries, one should be mindful of the influence these differences in lengths have when comparing the quantitative magnitudes.

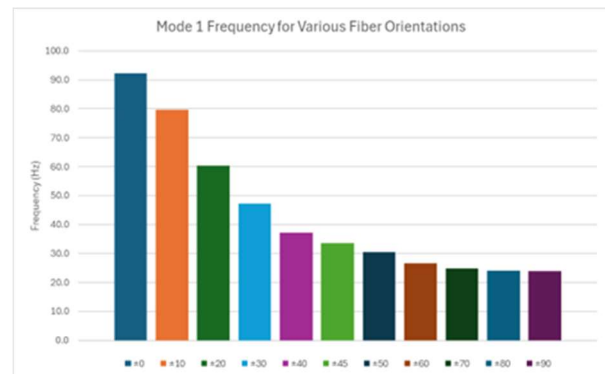


Figure 5. Mode 1 frequency for various fiber orientations of a rectangular laminate.

Half-Lenticular Boom

The half-lenticular geometry introduces curvature into the structure while maintaining an open cross section. The model was constructed by generating a curved shell, representing half of a lenticular profile, and applying the same boundary conditions and material properties as the flat laminate beam. The results are shown in Figure 6 below.

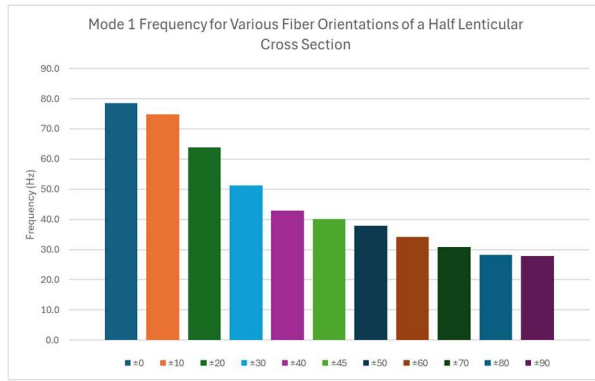


Figure 6. Mode 1 frequency for various fiber orientations of a half-lenticular cross-section.

Similar to the flat beam, the maximum natural frequency for the half-lenticular geometry occurred at $\pm 0^\circ$, reaching approximately 78.5 Hz. As the fiber orientation increased, the frequency decreased to approximately 28 Hz at $\pm 90^\circ$. However, the rate of decrease differed from that observed for the flat laminate.

This deviation suggests that curvature alters the stiffness contributions beyond those present in the flat case. In particular, the curved geometry introduces additional coupling between bending and in-plane deformation, enabling off-axis fibers to contribute more significantly to the structural response than in flat configurations. Despite this, axial alignment remained dominant in the open cross section geometry.

Full Lenticular Boom

The full lenticular geometry represents a closed cross section formed by joining two half-lenticular shells. This configuration introduces significant increases in both bending and torsional stiffness due to closed cross section.

Unlike both the flat and half-lenticular cases, the full lenticular geometry exhibited a shifted maximum first modal frequency. Shown in Figure 7, the maximum natural frequency does not occur at $\pm 0^\circ$, but instead at approximately $\pm 10^\circ$, reaching a peak value of 359.04 Hz. At $\pm 0^\circ$, the frequency is slightly lower at 351.54 Hz, indicating that purely axial fiber alignment is no longer optimal for maximizing stiffness.

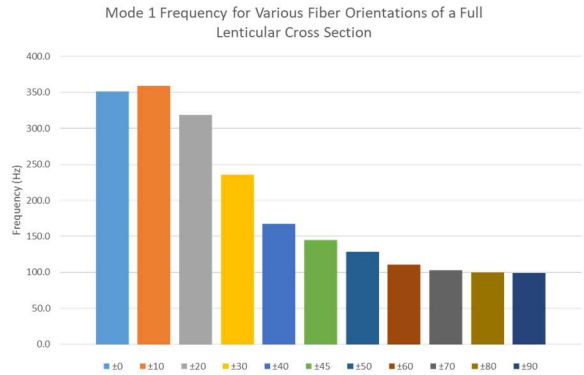


Figure 7. Mode 1 frequency for various fiber orientations of a full lenticular cross section.

This behavior is consistent with geometric coupling effects inherent to closed cross-section structures. The lenticular shape introduces interaction between bending, shear, and torsional deformation modes, allowing off-axis fibers to contribute to the structural response. As a result, a small degree of non-axial fiber alignment produced the highest first natural frequency in this configuration.

This finding is particularly significant as it demonstrates that traditional design intuition based on flat laminates does not directly apply to curved, closed cross-section composite structures.

Buckling Analysis

The effect of fiber orientation on buckling response was evaluated using linear eigenvalue analysis for only the full lenticular geometry, as this configuration represents the intended deployed structural configuration of the boom. For the study, a unit compressive load of 1 N was applied along the longitudinal axis of each geometry, and the resulting eigenvalues were used to determine critical buckling loads. Boundary conditions for this model applied a fixed condition in all degrees of freedom at one end of the boom, with the opposing end pinned (free to displace in the axial direction and rotate out of plane).

Full Lenticular Boom

The buckling response of the full lenticular geometry can be seen in Figure 8 and exhibits a non-monotonic relationship with fiber orientation. The maximum critical buckling load occurred at approximately $\pm 20^\circ$, reaching 4.76 kN, compared to 4.24 kN at $\pm 0^\circ$. Furthermore, the two highest buckling forces occur at non-axially aligned orientations, with $\pm 10^\circ$ reaching a critical buckling force of 4.75 kN.

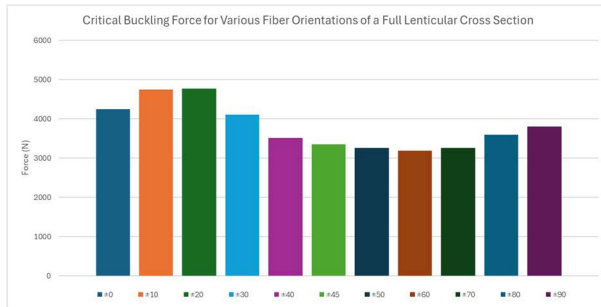


Figure 8. Critical buckling force for various fiber orientations of a full lenticular cross section.

This result indicates that axial fiber alignment does not maximize stability in the lenticular geometry. Instead, a combination of axial and off-axis fibers provides improved resistance to buckling. Off-axis fibers influence the buckling response by modifying the relative contributions of axial and shear stiffness.

The closed geometry further amplifies this effect by constraining deformation and distributing load across the cross-section. As a result, intermediate fiber orientations provide a more balanced stiffness distribution, leading to improved buckling performance.

Thermoelastic Deformation

Thermoelastic deformation was evaluated for the half-lenticular and full lenticular geometries, as these configurations capture the structural transition from open to closed cross sections. The analysis used a linear $\alpha \Delta T$ model to simulate the deformations arising during the cooldown from a processing temperature of 340°C to ambient 20°C conditions, capturing the deformation induced by anisotropic thermal contraction. Only $\pm 10^\circ$ fiber orientations were observed as they showed the highest first modal frequency and second highest critical buckling load for the full lenticular cross section.

Half Lenticular Boom

The half-lenticular geometry exhibited significant thermal deformation over the 330 mm length, with maximum displacement reaching approximately 6.5 mm. This large deformation is driven by the open cross section and lack of geometric symmetry.

In this configuration, anisotropic thermal strains generate unbalanced bending and twisting moments. The absence of an opposing structural surface prevents the cancellation of these strains, allowing the moments to manifest as large out-of-plane deformation. Additionally,

the reduced bending and torsional stiffness of the open section further amplifies the resulting deformation.

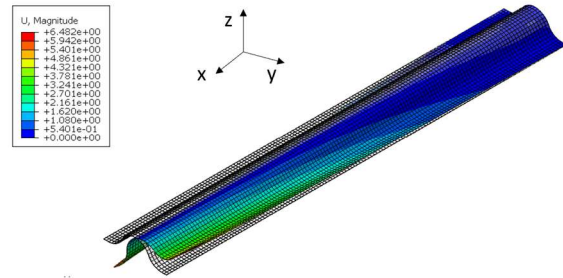


Figure 9. Thermally induced deformation of a half-lenticular beam with a $[-10/+10]$ layup. The black grid represents the undeformed geometry.

Full Lenticular Boom

In contrast to the half lenticular geometry, the full lenticular boom exhibited substantially reduced thermal deformation, with a maximum displacement of ~ 0.46 mm over the 330 mm length. This represents an order-of-magnitude reduction in thermally induced deformation.

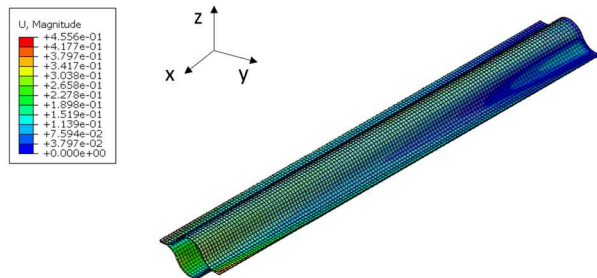


Figure 10. Thermally induced deformation of a full lenticular boom with a $[-10/+10]$ layup. The black grid represents the undeformed geometry.

The closed cross section provides geometric symmetry and increased stiffness, which is consistent with reduced sensitivity to anisotropic thermal strains. Opposing regions of the structure may offset thermally induced deformation, significantly reducing overall displacement.

This result highlights the critical role of cross-sectional geometry in controlling thermoelastic response and demonstrates the advantage of close cross-sectional designs for applications requiring high dimensional stability.

Tow Steered Finite Element Results

To evaluate the effectiveness of the proposed tow steering morphology described in the following section, the unmodified tow steering (TS) architecture with the outer $\pm 10^\circ$ plies for manufacturability ($[-10/+TS/-TS/+10]$) was implemented within the finite element framework and analyzed under the same loading conditions as the uniform laminate cases.

The tow-steered model was based on the full lenticular geometry, with spatially varying fiber orientations assigned element-by-element according to the prescribed steering pattern. The fiber architecture incorporated a combination of near-axial orientations ($\pm 10^\circ$) along the ridge and larger off-axis angles (up to $\pm 25^\circ$) toward the edges, as derived from the parametric study results. All boundary conditions and analysis procedures remained consistent with previous simulations, enabling direct comparison between uniform and tow-steered configurations.

To enable comparison between the manufactured tow-steered layup and the parametric study, two additional plies were added to each analyzed orientation as seen in Figure 11. Furthermore, the natural frequency analysis is restricted to fiber orientations up to $\pm 50^\circ$ as this region is of primary interest based on previous results. At the time of this paper's authorship, only half-lenticular studies have been completed for the tow-steered architecture.

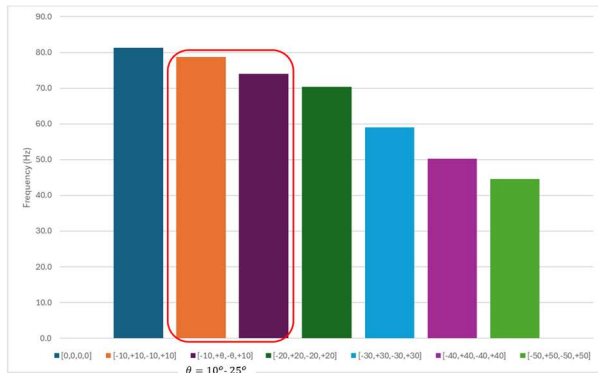


Figure 11. Mode 1 frequency of various fiber orientations for a half-lenticular cross section.

The tow-steered configuration maintained a first natural frequency comparable to the optimal uniform laminate case of $\pm 10^\circ$. This result is particularly significant as it demonstrates that tow steering can offer greater control over the deformed configuration without a significant reduction in the natural frequency.

The most significant improvement associated with the tow-steered architecture was observed in the thermoelastic response shown in Figures 12 and 13. For a four-ply laminate, thermally induced deformation was reduced from approximately 1.73 mm in the uniform, $\pm 10^\circ$, configuration to 0.64 mm in the tow-steered configuration. This represents a reduction of $\sim 63\%$ in maximum displacement.

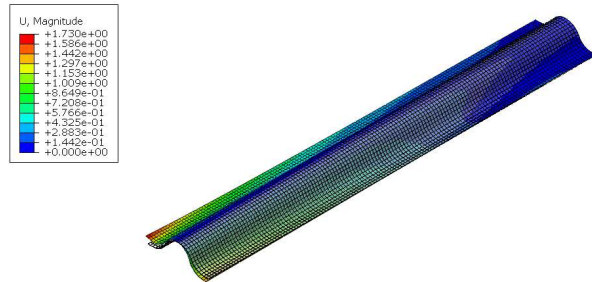


Figure 12. Thermally induced deformation of a half-lenticular boom with a $[-10/+10/-10/+10]$ layup. The black grid represents the undeformed geometry.

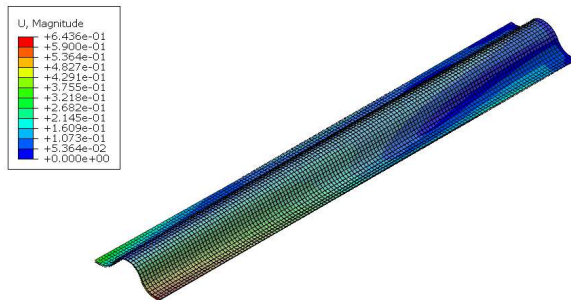


Figure 13. Thermally induced deformation of a half-lenticular boom with a $[-10/+TS/-TS/+10]$ layup. The black grid represents the undeformed geometry.

These initial results demonstrate that tow steering provides increased flexibility in balancing competing structural requirements. In uniform laminates, fiber orientation must be selected as a compromise between stiffness, buckling resistance, and thermal stability. In contrast, the tow-steered architecture allows these properties to be tailored simultaneously to a greater extent through spatial variation in fiber orientations, mitigating the tradeoff between competing structural requirements. By aligning fibers with local load paths and tailoring stiffness distribution across the cross section, tow steering provides a design approach for enhancing structural performance in deployable composite booms.

Tow-Steered Fiber Architecture Design and Implementation

Selection of Tow-Steering Morphology

The results of the parametric studies conducted on lenticular geometries directly informed the selection and development of the tow-steered architecture. These studies revealed that optimal structural performance does not occur at purely axial fiber orientations for enclosed lenticular geometries, but rather at intermediate angles that balance axial stiffness and shear compliance.

Specifically, the natural frequency analysis of the full lenticular geometry demonstrated that maximum dynamic stiffness occurs at approximately $\pm 10^\circ$ fiber orientation, while the buckling analysis showed that peak stability occurs near $\pm 20^\circ$. These results indicate that a combination of near-axial and off-axis fibers is required to simultaneously maximize bending stiffness and buckling resistance.

Based on these findings, a variable stiffness architecture was selected in which fiber orientations vary spatially across the width of the boom. The guiding design principle is to concentrate axially oriented fibers along the ridge of the lenticular cross section to maximize bending stiffness, while fibers with larger off-axis angles are introduced along the edges to enhance shear resistance and mitigate torsional deformation.

To implement this concept, two primary steering angles were defined: (i) a mid-region steering angle of $\pm 10^\circ$, corresponding to the optimal orientation for maximizing natural frequency and (ii) an edge-region steering angle of approximately $\pm 25^\circ$, selected to approximate the enhanced buckling resistance seen at $\pm 20^\circ$ while also increasing off-axis fiber content to improve performance in shear.

This combination enables a smooth transition in stiffness across the boom, producing a tailored structural response that leverages both axial and shear-dominated behavior.

Parametric Definition of Tow-Steered Paths

The tow-steered fiber paths were defined using a formulation based on discrete spatial coordinates. Each fiber path is described by a set of (x, y, t) values, where x and y define the position of the tow within the boom, and t defines the local fiber orientation.

The variation in fiber orientation across the width of the boom was generated using a modified tangent-based

formulation, where the local slope of the fiber path is governed by the prescribed steering angle. This allows the fiber orientation to vary continuously across the width of the structure, enabling smooth transitions between regions of varying stiffness.

The x-coordinate was defined as an evenly spaced vector spanning the width of the boom, while the y-coordinate was incrementally calculated based on the local fiber angle and x-coordinate. This approach ensures that the resulting tow steering paths remain continuous and manufacturable, while also providing precise control over local fiber orientation.

Using this method a set of tow-steered guidepaths were generated that reflect the desired stiffness distribution across the lenticular geometry. The resulting morphology, shown in Figures 14 and 15, exhibits increased fiber density along the ridge and more pronounced angular variation near the edges, consistent with the intended structural behavior.

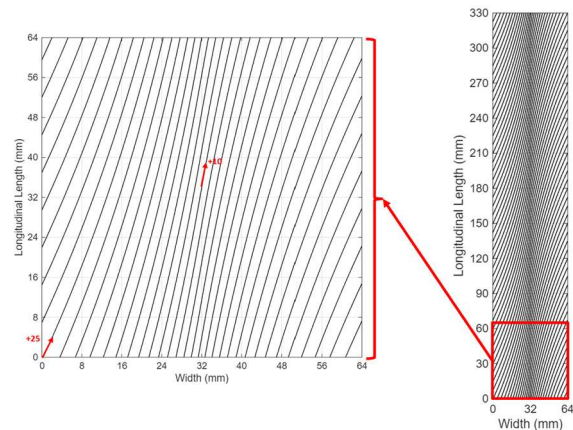


Figure 14. Single ply tow-steered architecture

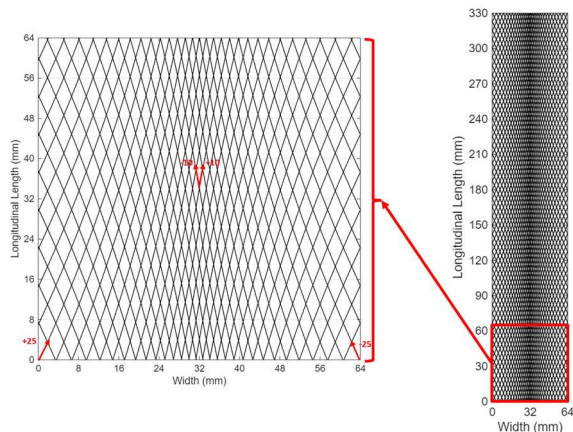


Figure 15. Two ply tow-steered architecture

Implementation in the Finite Element Model

To incorporate the tow-steered fiber architecture into the finite element model, a scripting-based approach was developed to assign fiber orientations and composite layups at the mesh element level within Abaqus CAE.

The lenticular boom model was discretized into a structured mesh consisting of 142 element rows along the axial direction. Each row corresponds to a distinct region of the composite layup, allowing for spatial variation in fiber orientation along the length of the boom. Within each row, elements spanning the width of the cross section were grouped into sets corresponding to their position relative to the ridge and edges of the geometry.

A python-based scripting workflow was implemented to automate the assignment of composite layups and fiber orientations. For each element set, the script performs the following operations: (i) defines a composite layup with the appropriate number of plies and material properties, (ii) assigns a local coordinate system aligned with the geometry of the boom, (iii) applies a fiber orientation angle corresponding to the prescribed tow-steering pattern.

This approach enables the direct mapping of the parametric tow-steering guidepaths onto the finite element mesh, ensuring that each element reflects the intended local fiber orientation. By automating this process, the model can accommodate complex variable stiffness architectures that would be impractical to define manually. The use of scripting is particularly critical given the spatial resolution of the model. With over 100 distinct regions requiring unique fiber orientations, manual assignment would be both time-consuming and error prone. The automated workflow ensures consistency across the model and allows for rapid iteration of tow-steering designs.

Consideration of Manufacturing Constraints

While the finite element implementation allows for continuous variation in fiber orientation, practical realization of these tow-steered architectures is constrained by the capabilities of AFP systems.

The AFP machine used to manufacture the tow-steered architecture deposits fiber tows in discrete groups of 8 following a prescribed guidepath. The center of the tow group follows the programmed trajectory, while the outer tows deviate slightly due to their finite width. This results in the formation of gaps or overlaps

between adjacent tow groups, introducing local variations in fiber volume fraction and thickness.

Additionally, there are limitations on the curvature of tow paths that can be achieved without inducing defects such as wrinkling or loss of adhesion to the build surface [5]. These constraints restrict the range of allowable steering angles and require careful consideration when translating idealized fiber paths into manufacturable designs.

Due to these limitations certain adaptations were made to the tow-steered architecture for manufacturing: (i) deviation from the prescribed guidepath along the outer tows within the tow group were accepted and both no-gap and no-overlap configurations were fabricated to experimentally determine their effects on structural performance, (ii) unidirectional $\pm 10^\circ$ plies were added outside of the two tow-steered plies to provide sufficient tack to the AFP build plate creating the layup [-10/+TS/-TS/+10], (iii) the tow steered pattern would be fabricated into thermoplastic panels that would later be formed into the lenticular geometry through thermostamping. These adaptations resulted in the tow-steered panels seen in Figures 16 and 17.

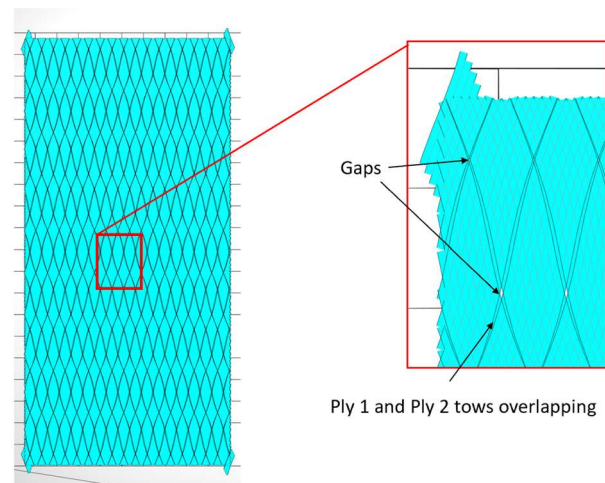


Figure 16. Simulated tow paths for a no-overlap configuration tow-steered panel

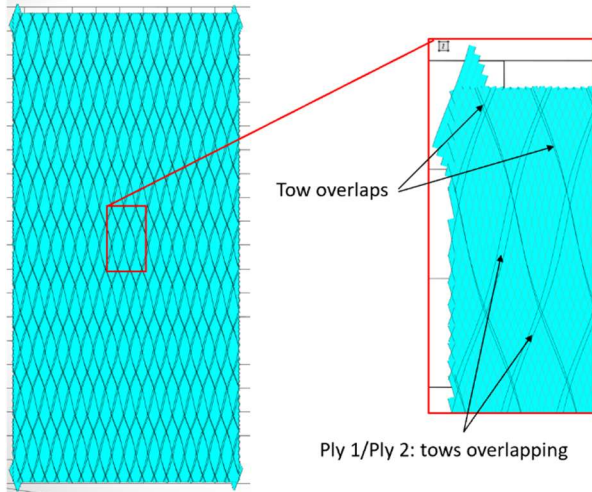


Figure 17. Simulated tow paths for a no-gap configuration tow-steered panel

Conclusion

This study presented a comprehensive investigation into the role of fiber orientation and structural geometry on the performance of thin-ply thermoplastic composite booms for small satellite applications. Through a systematic finite element analysis of flat, half-lenticular, and full lenticular geometries, it was shown that traditional design intuition based on axial fiber alignment does not extend to closed-section structures. While flat and open geometries exhibited maximum stiffness at $\pm 0^\circ$, the full lenticular configuration demonstrated optimal dynamic and buckling performance at off-axis fiber orientations (approximate $\pm 10^\circ$ to $\pm 20^\circ$), consistent with coupling between axial, shear, and torsional deformation modes.

The results further demonstrated that closed cross-sectional geometry plays a dominant role in enhancing structural efficiency, significantly increasing stiffness and reducing thermoelastic deformation compared to open configurations.

The implementation of a tow-steered laminate architecture showed that spatially varying fiber orientations can improve structural performance relative to the uniform laminates evaluated in this study. These findings underscore the importance of integrated geometry-material design and suggest that tow steering is a promising approach for improving deployable composite structures. Future work will focus on experimental validation and the incorporation of manufacturing constraints and imperfections into the modeling framework.

References

- [1] Bouzoukis, Konstantinos-Panagiotis, et al. "An overview of CubeSat missions and applications." *Aerospace*, vol. 12, no. 6, 16 June 2025, p. 550, <https://doi.org/10.3390/aerospace12060550>.
- [2] Imbriale, William A. "Space antenna handbook." (2012).
- [3] "UK SPACE COMPANIES' PARTNERSHIP COMPLETED THE DEVELOPMENT OF AN ADVANCED DEPLOYABLE SAR ANTENNA PAYLOAD." News and Blogs, Oxford Space Systems, [oxford.space/post/?permalink=uk-space-companies-partnership-completed-the-development-of-an-advanced-deployable-sar-antenna-payload](https://www.oxford-space.com/news-and-blogs/uk-space-companies-partnership-completed-the-development-of-an-advanced-deployable-sar-antenna-payload). Accessed 5 Apr. 2026.
- [4] Wilkie, Keats. "The NASA Advanced Composite Solar Sail System (ACS3) Flight Demonstration: A Technology Pathfinder for Practical SMALLSAT Solar Sailing - NASA Technical Reports Server (NTRS)." NASA, NASA, Aug. 2021, ntrs.nasa.gov/citations/20210016824.
- [5] "Packaging and Deployment of Solar Arrays and Antennas - Sergio Pellegrino." Caltech, www.pellegrino.caltech.edu/packaging-and-deployment-of-solar-arrays-and-antennas. Accessed 5 Apr. 2026.
- [6] Rousseau, Guillaume, et al. "Automated Fiber Placement Path Planning: A state-of-the-art review." *Computer-Aided Design & Applications* 16.2 (2019).
- [7] Belvin, Keith W., et al. "Advanced Deployable Structural Systems for Small Satellites - NASA Technical Reports Server (NTRS)." NASA, NASA, ntrs.nasa.gov/citations/20170003919. Accessed 5 Apr. 2026.
- [8] Fernandez, Juan M. "Advanced deployable shell-based composite booms for small satellite structural applications including solar sails." *International symposium on solar sailing 2017*. No. NF1676L-25486. 2017.
- [9] Krueger, Ronald, and Andrew Bergan. "Advances in thermoplastic composites over three decades—a literature review." (2024).